Measured and modelled low field relative permeability for dual phase steels at high temperature

L. Zhou[a*], R.Hall[a] and C. L. Davis[a]

[a] *University of Warwick, Warwick Manufacturing Group (WMG), Coventry, CV4 7AL, UK*

** Corresponding author. Tel.: +44247 6523905*

E-mail address: Lei.zhou@warwick.ac.uk (L.Zhou)

Abstract

The magnetic properties of steels are sensitive to temperature and currently the only way to determine them is by experimental measurement. In this work a cylindrical shaped ceramic cored EM sensor has been used to measure the low magnetic field inductance of pure iron and C-Mn steels with ferrite + pearlite microstructures during heat treatment up to 800 ℃ in a furnace. The low field relative permeability values have been determined by fitting the sensor readings to a finite element sensor model generated in COMSOL, where the model has been validated for room temperature measurements using samples of known low field relative permeability. The low field relative permeability values with temperature follow the expected trend of increasing values with temperature, particularly close to the Curie temperature. The measured low field relative permeability values for the mixed ferrite + pearlite microstructures have been compared to predicted values from an FE microstructure-permeability model using the single phase (ferrite or pearlite) low field relative permeability values as input. The model predictions agree well with the experimentally measured values allowing any two-phase ferrite + pearlite microstructure low field relative permeability with temperature relationship to be determined. The model has also been used to determine the low field relative permeability of ferrite + austenite microstructures with temperature.

Keywords: High-temperature relative permeability; Steel; EM sensors; In-situ test; Phase fraction; Finite element analysis

1. Introduction:

It is known that temperature has a strong effect on the magnetic properties of iron and steel, with an increase in permeability of iron being seen for low applied magnetic fields until close to the Curie temperature, although differing rates of increase with temperature, and temperature of maximum permeability, are seen based on the applied field [1]. It has been reported that the rate of increase in the permeability with temperature in steels depends on the steel grade and also the applied field [2,3] although there is limited data available in the literature and there are no models available for predicting properties at elevated temperatures with respect to microstructure.

General approaches exist for modeling the effective magnetic (or electrical) properties in a material that has two components with contrasting properties: the effective medium theory. The principle of the effective medium theory is that the electrical/magnetic potential due to the mixture placed in the external electrical/magnetic field is equal to the potential caused by a geometrically identical object having an effective conductivity/permeability/permittivity. Empirically based power law models have been popularly used [4–7]. The power law model predicts the effective permeability as

$$\mu_e{}^{\beta} = (1-f)\mu_1{}^{\beta} + f\mu_2{}^{\beta} \qquad (1)$$

Where μ_1 and μ_2 are the relative permeability values of the first and second phase respectively, f is the fraction of the second phase, and β is a dimensionless parameter. Examples of the power law are the Birchak formula (β = 1/2) [7] and the Looyenga formula (β = 1/3) [6] for prediction of the dielectric constant of mixtures.

Hao et al. developed a FE microstructure-permeability model to predict the low field relative permeability based on actual microstructures in steels [4]. The microstructural phases were considered as constituents with different low field relative permeability values. The FE microstructure model was found to give good agreement with measured results over the whole range of ferrite fraction for austenite/ferrite stainless steel microstructures at room temperature, whilst the power-law model with $\beta = 1/2$ did not give a good fit, and using $\beta = 1/3$ only gave good agreement with measured results at ferrite fractions above 40% (samples with ferrite fractions below 40% would require a much smaller β value to give good fitting) [4]. This is because when the ferrite fraction is low (ferrite grains are isolated), the magnetic flux takes a complex route between ferrite regions, to minimize passage in austenite. The empirically based power law models do not consider this effect, hence are not able to fit well throughout the full ferrite fraction range using one β value. Using the same FE modelling approach, Zhou et al. extended the model to consider 3D microstructures and modelled the effect of ferrite fraction on the low field relative permeability of ferrite/pearlite steels with both uniform and non-uniform second phase distributions and showed very good fit to the experimental data [8,9]. It was reported that the shape of the permeability-ferrite fraction relationship in ferrite/pearlite microstructures is different than for ferrite/austenite microstructures due to the fact that the magnetic flux pathway is less affected by the second phase when the latter is ferromagnetic (e.g. pearlite, bainite, martensite and/or tempered martensite), than when it is paramagnetic (austenite) [8]. To date, the FE microstructure modelling to predict relative permeability has only been considered for samples at room temperature.

Commercial low magnetic field EM sensors, such as the EMspec system [10], have recently been developed to monitor phase transformation in strip steels after hot rolling on the run out table. The sensors detect the difference in electromagnetic properties, i.e. relative permeability

and electrical conductivity, in the steels with different microstructural phase balances (for example ferrite and austenite during transformation). For quantitative characterization of the microstructure accurate low field relative permeability and electrical resistivity with temperature data is required. Electrical resistivity with temperature is well reported in the literature [11] whereas there is little data on low field permeability data, and none for ferrite and austenite microstructures at high temperature.

In this paper, a cylindrical shaped ceramic EM sensor has been used to measure the inductance of pure iron and C-Mn steels with ferrite + pearlite microstructures at temperatures up to 800 ℃ in a furnace. The measured inductance and resistivity values from the literature have been used to obtain low field relative permeability values with respect to temperature. The low field relative permeability values for the single phase microstructures of ferrite or pearlite have been used in a microstructure-permeability model to predict the low field relative permeability values for two phase ferrite + pearlite microstructures with temperature, which have been compared to measured values. The model has also been used to predict the low field relative permeability values for ferrite + austenite microstructures with temperature.

2. Materials and method

Melting grade (pure) iron and hot rolled C-Mn steels with different carbon contents, full compositions given in Table 1, were used in the work.

Table 1. Chemical composition for the steel samples used in this work, all in wt%.

	C	**Si**	**Mn**	**S**	**P**	**Cu**
0.17C	0.17	0.28	0.80	0.03	0.01	0.09
0.38C	0.38	0.26	0.75	0.03	0.02	0.12

0.80C	0.80	0.20	0.96	0.03	0.02	0.02

Metallographic samples were taken in the transverse direction of the supplied steels (plate or bar stock), polished to an OPS finish and etched in 2% nital. The samples were imaged using a Zeiss Akioskop-2 optical microscope equipped with Axiovision 4.6.3 image capture software. The ferrite fraction and ferrite grain size of the samples were analysed using "Image J" image analysis software.

Samples for EM measurements (cylindrical shape with 10mm diameter and 110mm length) were machined from the as-received steel, accurate sample size measurements were made using vernier calipers for input into the FE model. The high temperature EM sensor, which was formed around an alumina former, has an exciting coil of 50 turns and sensing coil of 54 turns. In order to withstand the high temperatures K-Type thermocouple wire was used. The sensor was encased in a high temperature solid silica coating, which both protects the exciting and sensing coils as well as holds them in place. Images of the high temperature cylindrical sensor during construction are shown in Figure 1. The coils were driven by a frequency response analyser (SL1250) at 100 Hz, and the real inductance values were determined from mutual inductance measurements. The frequency used was selected to be as low as possible without sacrificing the stability of the data measured (as the induced voltage increases with frequency) as then the inductance measured is mainly affected by the low field relative permeability, rather than resistivity (as the effects of eddy currents on the signal is small).

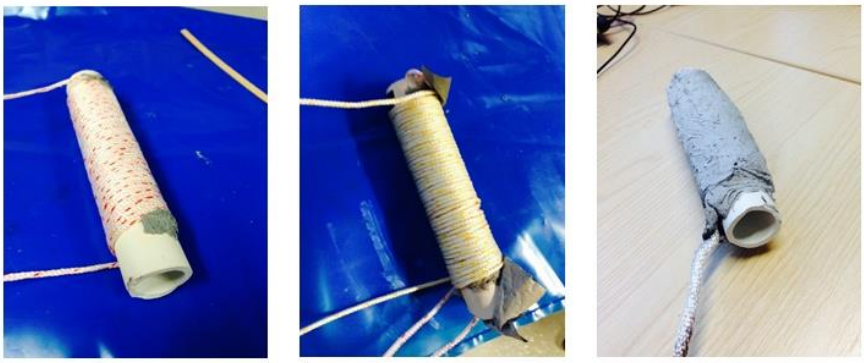

a) b) c)

Figure 1: High temperature EM sensor in different stages of construction a) showing the alumina former (26mm outer diameter and 145mm length) and exciting coil, b) sensing coil wound over the exciting coil and c) sensor encased in a silica coating.

The high temperature EM sensor was used to measure the inductance of the pure iron and C-Mn steels during heating up to 800 ℃ in a Carbolite Gero RHF1500 muffle furnace at a heating rate of 6.5 $^{\circ}$C min^{-1}. The temperature of the sample was measured separately by a K type thermocouple which was spot welded to the sample. EM sensor measurements were carried out at room temperature to confirm that the effect of thermocouple attachment to the sample on the EM sensor signal is negligible.

Electrical resistivity measurements were performed at room temperature using a conventional four-point DC method with a Cropico DO5000 microohmmeter. Each resistivity value was determined by taking the average of 10 measurements on the same sample used for EM sensor measurements. The resistivity change with temperature for the different samples were obtained from [11]. The relative permeability values were determined by fitting the modelled real (as in not imaginary) inductance with the experimental measured real ones for samples of known permeability at room temperature, based on a nonlinear least square method in Comsol LiveLink for Matlab. Close fits (less than 1% error) between the modelled and measured real inductance for all the samples have been achieved. Then the relative permeability values for

the high temperature data was determined from the model using the high temperature resistivity values and measured inductance values. The fitting method is described in [12]. The model predicted an applied magnetic field of 26 A/m at the sample position, which agrees well with the measured field (measured using a Gauss meter). This field strength is similar to the applied field of the commercial EMspec sensor in the sample, when operating at its standard 40mm lift-off to the sample.

3. Results and discussion

3.1 Microstructures

Optical microstructures of the pure iron, 0.17C, 0.38C, and 0.8C as-received samples are shown in Figure 2. Table 2 shows a summary of the average ferrite grain size (ECD), ferrite percentage and resistivity, with standard deviation values, for the samples. The resistivity value increases with carbon content in the C-Mn steels due to the increasing pearlite content and is also higher in the C-Mn steels compared to the pure iron due to the presence of alloying elements (Si and Mn) and the smaller grain size, as well as the presence of pearlite.

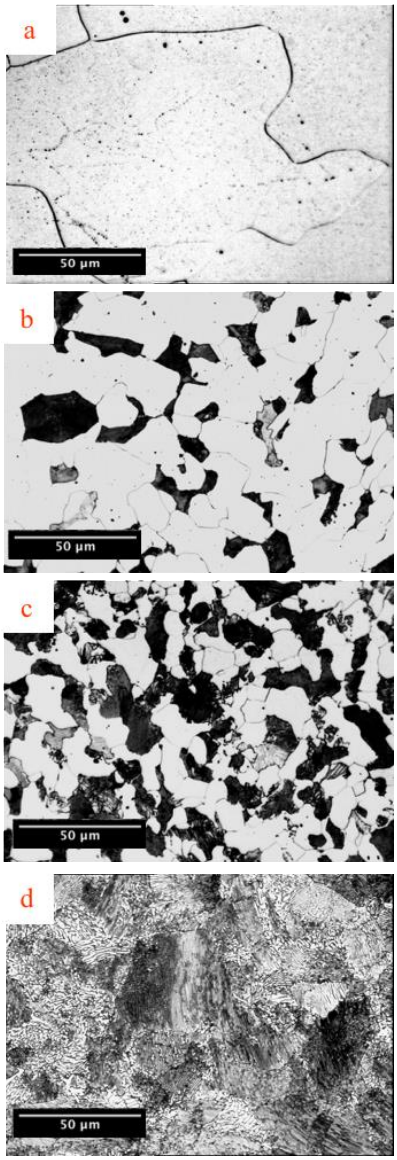

Figure 2. Optical microstructures of a) pure iron, b) 0.17C, c) 0.38C, and d) 0.8C as-received samples.

Table 2. Summary of the ferrite percentage, ferrite grain size and resistivity values for the pure iron and C-Mn steels. Error bars are in standard deviation.

Sample	**Average ferrite grain size (µm)**	**Ferrite%**	**Resistivity (nΩm)**
Pure iron	155 ± 68.1	100	104.0 ± 0.3
0.17C	24.5 ± 10.7	70.8 ± 1.8	210.9 ± 0.1
0.38C	14.0 ± 5.8	48.9 ± 1.2	218.6 ± 0.2
0.8C	-	0	243.7± 0.3

3.2 EM measurements

EM sensors exploit the difference in electromagnetic properties, such as relative permeability and electrical conductivity, between samples with different microstructural phase balances. In ferromagnetic steels, the low frequency real inductance values are mainly affected by the changes in relative permeability whilst at increasing frequency the effect of eddy currents (and hence the resistivity of the steels) affects the signal. Real inductance values with frequency for the four steels, measured at room temperature using an EM sensor using with multi-frequency analyser, are shown in Figure 3 [8]. It can be seen that the C-Mn steels show a plateau in real inductance values at low frequency when the effect of eddy currents is negligible, however the pure iron sample still shows an increasing real inductance with decreasing frequency as its lower resistivity means that eddy currents have a greater effect at low frequency. Therefore, the inductance values measured at 100 Hz at room temperature do not simply follow an order based on the expected relative permeability values for the samples. Whilst inductance measurements at 10 Hz would give the expected ranking of samples based on their relative permeability values, as the pure iron sample has not reached a plateau value any simple approximation between the inductance and relative permeability would be incorrect. Sensor measurements as very low frequency (<10 Hz) were found to be inaccurate as the low voltage meant that significant noise in the signal was observed, particularly at high temperatures. Therefore an FE model for the sensor – sample system to determine the relative permeability values from the measured inductance taking into account the influence of resistivity is essential.

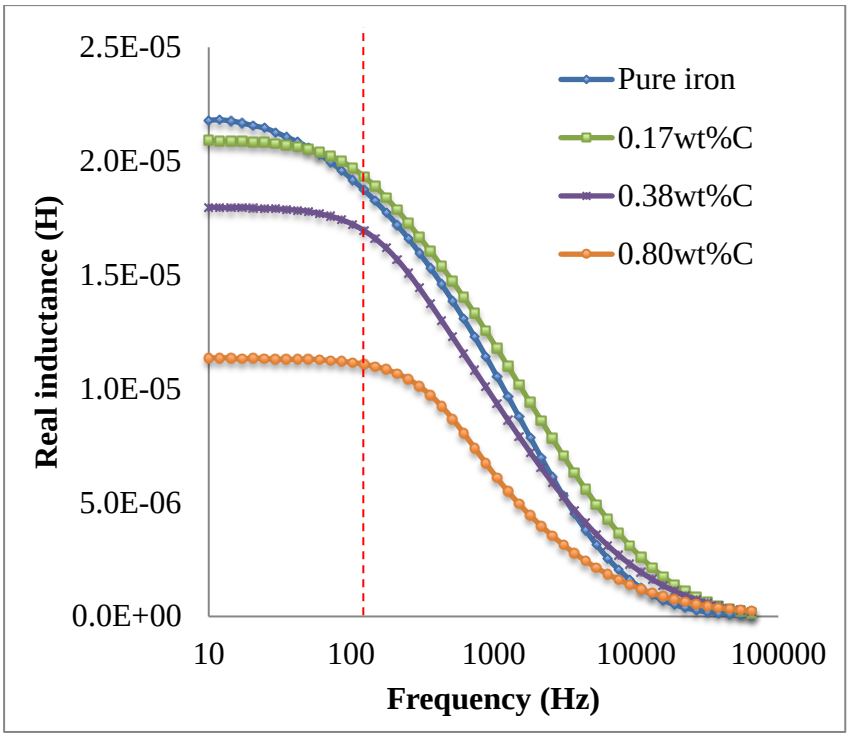

Figure 3. Real inductance changes with frequency for pure iron, 0.17C 0.38C and 0.80C steel samples [8].

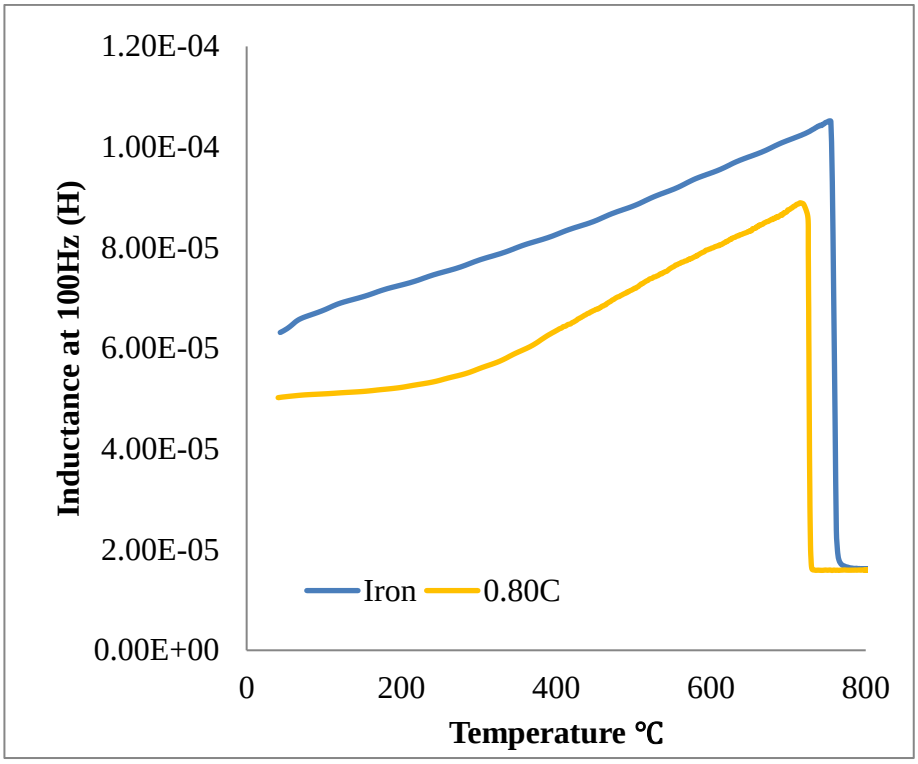

Figure 4. Real inductance at 100 Hz changes with temperature for pure iron and 0.8C steel samples.

The measured real inductance values at 100Hz versus temperature for the pure iron and 0.8C steel samples, using the high temperature EM sensor, are shown in Figure 4. The real inductance values increase with temperature until the Curie point is reached at around 750 – 780°C, then decreases to a very low value. The Curie point for the more alloyed 0.8C steel is lower than for the pure iron sample as expected [13]. The relative permeability values for the pure iron (100% ferrite) and 0.8C steel (100% pearlite) sample, calculated from the FE model of the cylindrical sensor, are plotted against temperature in figure 5. The relative permeability value for pure iron agrees well with Bozorth, who reported that the relative permeability of iron at 700 °C increases from 2800 at 16 A/m to 7100 at 40 A/m, then gradually decreases to 3100 at 240A/m [1]: the reported relative permeability change with applied field strength is plotted in Figure 6. The relative permeability value is about 4700 at 26 A/m (assuming a best fit line), compared to the determined relative permeability value of 4400 at 700 °C in this study.

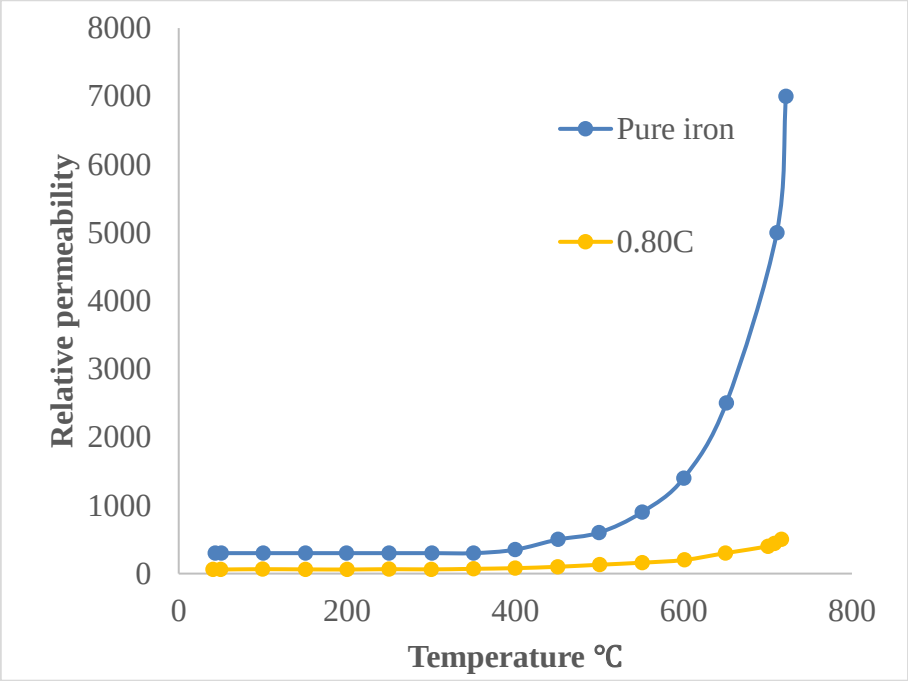

Figure 5. Relative permeability change with temperature for pure iron and 0.8C steel samples.

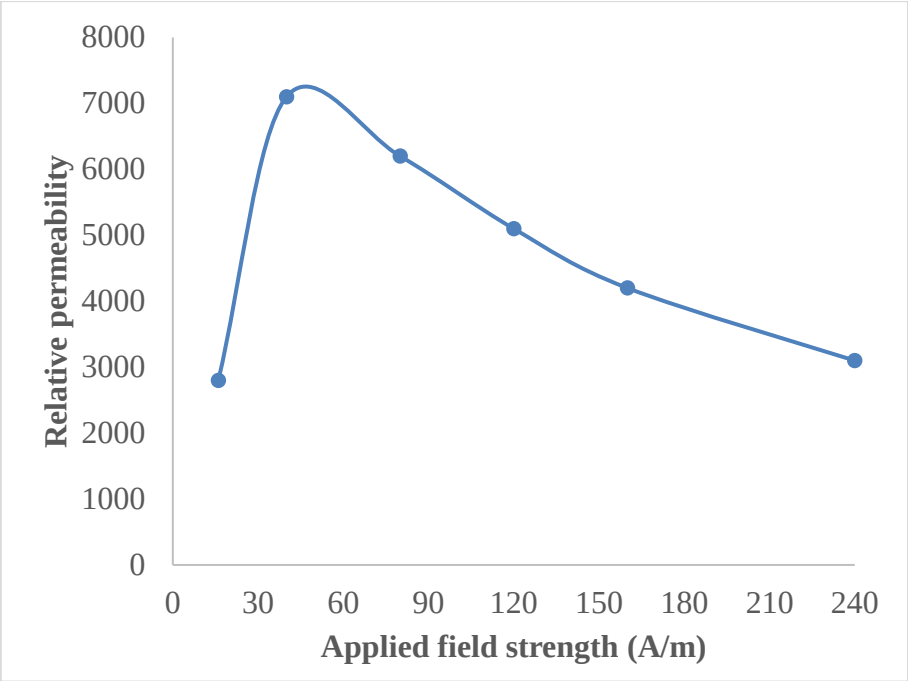

*Figure 6. Relative permeability change with applied field for pure iron sample at 700 °C, replotted data from **[1]***

4. FE microstructure – permeability model

The COMSOL FE microstructure - permeability model used in this study is similar to that used by Hao et al with conditions that the top and bottom boundaries of the sample were set with a magnetic potential of 1 and 0, respectively, to generate a uniform horizontal magnetic field. The left and right boundaries of the sample were set as electric insulation (magnetic field normal to the boundary) to eliminate the demagnetising field [4]. The boundary conditions of the model are shown in Figure 8. Greyscale optical micrographs of the ferrite/pearlite microstructures with different ferrite fractions were converted to black and white binary images and imported into the COMSOL model.

The determined relative permeability values of pearlite and ferrite with temperature (shown in Figure 5) were used as an input into the microstructure model for the appropriate

microstructural regions. The effective relative permeability of the mixture was then calculated by:

$$\mu_e = \frac{B_{ave}}{\mu_0 H_{ave}} \qquad (2)$$

Where B_{ave} is the average flux density inside the sample, μ_0 is the permeability of free space, and H_{ave} is the average magnetic field inside the sample.

The FE microstructure modelled results of the relative permeability change with temperature compared with the experimentally determined values for the ferrite + pearlite microstructures (0.17C and 0.38C steels) are shown in Figure 7. It can be seen that the FE modelled permeability values give very good agreement with the experimental obtained data.

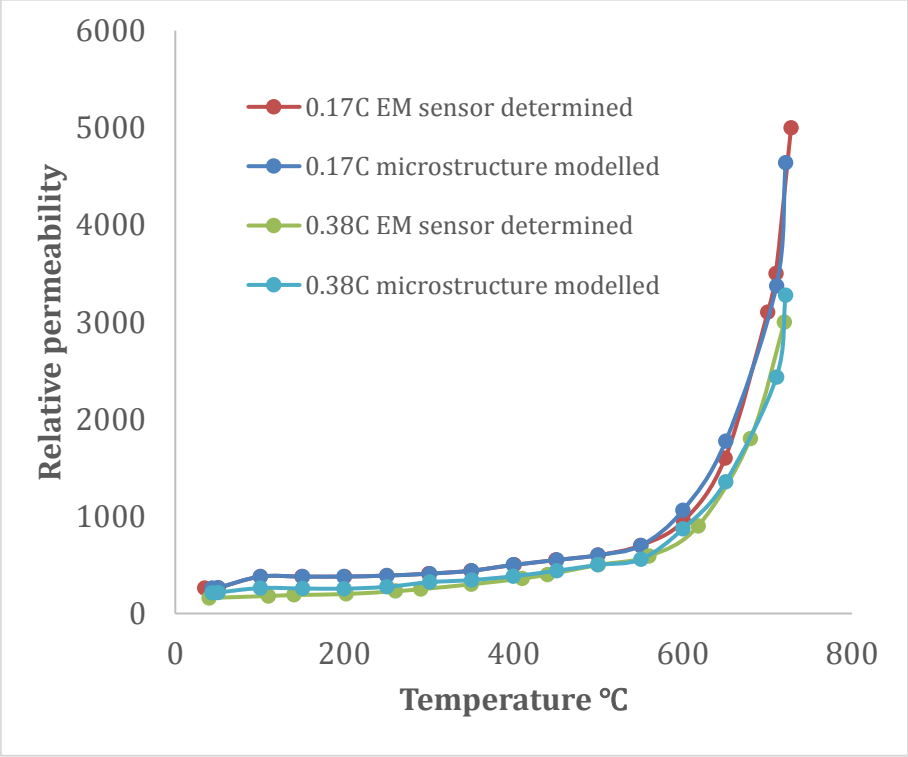

Figure 7. Relative permeability change with temperature for 0.17C and 0.38C ferrite + pearlite steel samples compared to the FE microstructure modelled results.

Example magnetic flux line – microstructure models are given in Figure 8 for the 0.38C steel at 100°C and 720°C where it can be seen that at the higher temperature the magnetic flux concentrates more in the ferritic regions compared to the lower temperature simulation. This is due to the greater difference in relative permeability between ferrite and pearlite at the higher temperature and therefore the greater preference for magnetic flux to be in the ferritic regions. As discussed earlier, the FE microstructure model works better than the power law models at room temperature for two phase microstructures, particularly ferrite and austenite where there is a large difference in relative permeability values. The current study suggests that this will be even more the case at high temperatures for these ferrite and pearlite microstructures as well as ferrite and austenite structures.

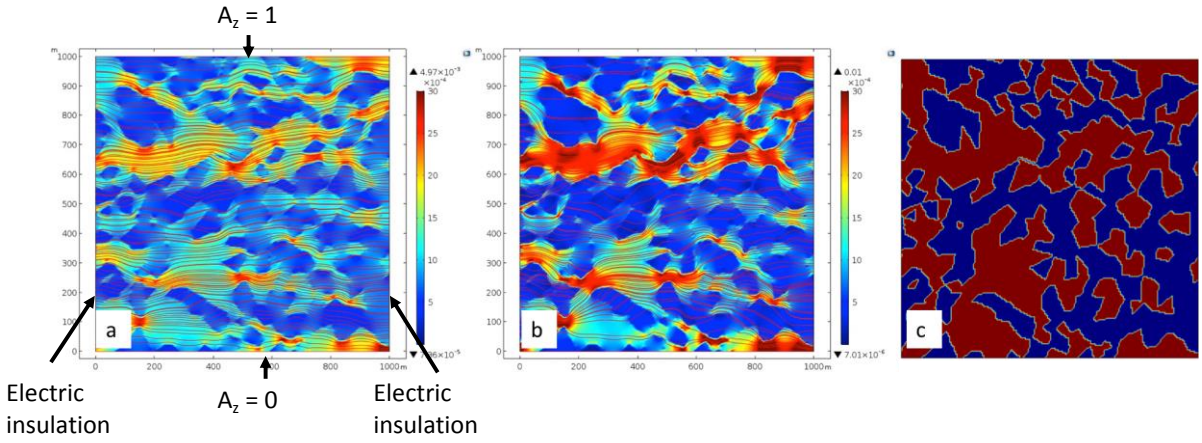

Figure 8. FE modelled results of magnetic flux distribution for the 0.38C steel at (a) 100°C and (b) 720°C (Stream line: magnetic flux density, boundary condition labelled in (a)). c) processed micrograph showing phase distribution of ferrite (red) and pearlite (blue).

The low field relative permeability values for mixed ferrite + austenite microstructures over the range of 0-100 % ferrite fraction were predicted for the temperature range of 451°C to 721°C using the microstructure permeability model, Figure 9. This temperature range was selected as being relevant for phase transformation from austenite to ferrite (or other ferromagnetic phases such as bainite, pearlite, martensite) during dynamic cooling, such as on the run out table after

hot rolling of steel strip. It can be seen that the low field permeability starts to show an increase at around 40-50% ferrite, where the ferrite phase is starting to be linked and form a continuous magnetic flux pathway. This has been reported before for ferrite + austenite at room temperature [4]. A more significant increase happens at around 70% ferrite, where most of the ferrite phase is interconnected. These low field permeability values can be used to quantitatively predict phase transformation fraction from low field EM sensor signals, such as EMspec system [14–16].

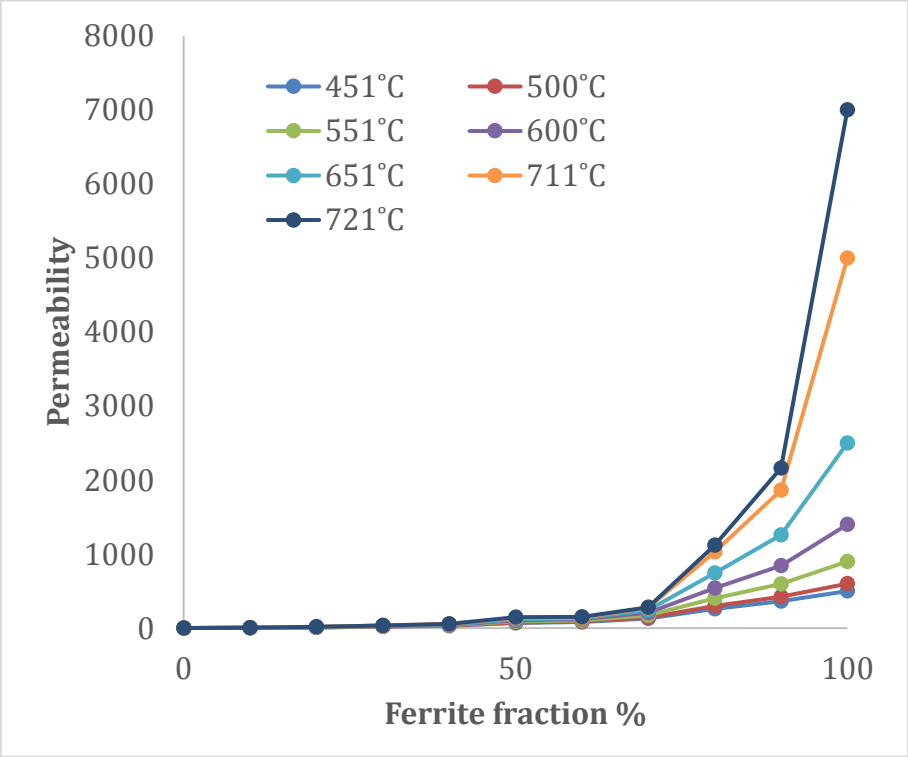

Figure 9. Low field relative permeability values for mixed ferrite + austenite microstructures over the range of 0-100 % ferrite fraction at temperature range of 451°C to 721°C

5. Conclusions

High temperature low field relative permeability values have been determined for pure iron (100% ferrite microstructure), 0.17C and 0.38C steels (ferrite and pearlite microstructures) and 0.8C steel (100% pearlite microstructure) from cylindrical sensor measurements of inductance and a sensor-sample FE model, taking into account changes in resistivity with temperature. A FE microstructure-permeability model was used to predict the relative permeability of the dual-phase (ferrite + pearlite) steel microstructures at different temperatures up to Curie point using as input the single phase microstructure relative permeability values. The model predictions agree very well with the experimentally measured ones. Therefore it is proposed that the high temperature permeability of any dual phase microstructure can be predicted and results for ferrite and austenite microstructures are presented. Based on these (measured or predicted) high-temperature permeability values, known resistivity with temperature data and the microstructure-permeability models, it is possible to use low field EM sensors to determine the ferrite fractions for dual phase steels at any temperature below the Curie point.

Acknowledgements

The authors would like to thank WMG for the provision of experimental facilities, EPSRC for funding under grant EP/K0279561/1 and, with Tata Steel, funding via an Industrial CASE studentship.

References

[1] R.M. Bozorth, Ferromagnetism, Van Nostrand, 1965.

[2] C.W. Burrows, Correlation of the magnetic and mechanical properties of steel, Bull. Bur. Stand. 13 (1916) 173. doi:10.6028/bulletin.298.

[3] N. Takahashi, M. Morishita, D. Miyagi, M. Nakano, Examination of Magnetic Properties

of Magnetic Materials at High Temperature Using a Ring Specimen, IEEE Trans. Magn. 46 (2010) 548–551. doi:10.1109/TMAG.2009.2033122.

[4] X.J. Hao, W. Yin, M. Strangwood, A.J. Peyton, P.F. Morris, C.L. Davis, Modelling the electromagnetic response of two-phase steel microstructures, NDT E Int. 43 (2010) 305–315. doi:10.1016/j.ndteint.2010.01.006.

[5] W. Yin, A.J. Peyton, M. Strangwood, C.L. Davis, Exploring the relationship between ferrite fraction and morphology and the electromagnetic properties of steel, J. Mater. Sci. 42 (2007) 6854–6861. doi:10.1007/s10853-006-1327-6.

[6] H. Looyenga, Dielectric constants of heterogeneous mixtures, Physica. 31 (1965) 401–406. doi:10.1016/0031-8914(65)90045-5.

[7] J.R. Birchak, C.G. Gardner, J.E. Hipp, J.M. Victor, High dielectric constant microwave probes for sensing soil moisture, Proc. IEEE. 62 (1974) 93–98. doi:10.1109/PROC.1974.9388.

[8] L. Zhou, J. Liu, X.J. Hao, M. Strangwood, A.J. Peyton, C.L. Davis, Quantification of the phase fraction in steel using an electromagnetic sensor, NDT E Int. 67 (2014) 31–35. doi:http://dx.doi.org/10.1016/j.ndteint.2014.06.007.

[9] L. Zhou, C.L. Davis, P.J.J. Kok, F. van den Berg, Magnetic NDT for Steel Microstructure Characterisation – Modelling the Effect of Second Phase Distribution on Magnetic Relative Permeabilty, WCNDT. (2016).

[10] F.V.-B. H. Yang A. Luinenburg, C. Bos, G. Kuiper, J. Mosk, P. Hunt, M. Dolby, M. Flicos, A. Peyton, C. Davis, In-Line Quantitative Measurement of Transformed Phase Fraction by EM Sensors during Controlled Cooling on the Run-Out Table of a Hot Strip Mill, WCNDT. (2016).

[11] ASM Handbook, Volume 1: Properties and Selection: Irons, Steels, and High-Performance Alloys, ASM International, 2017.

[12] J. Liu, X.J. Hao, L. Zhou, M. Strangwood, C.L. Davis, A.J. Peyton, Measurement of microstructure changes in 9Cr–1Mo and 2.25Cr–1Mo steels using an electromagnetic sensor, Scr. Mater. 66 (2012) 367–370. doi:http://dx.doi.org/10.1016/j.scriptamat.2011.11.032.

[13] K. Ara, Magnetic characteristics of ferromagnetic stainless steels, IEEE Trans. Magn. 25 (1989) 2617–2623. doi:10.1109/20.24500.

[14] J. Shen, L. Zhou, W. Jacobs, P. Hunt, C. Davis, Real-time microstructure control using EMspec sensor, in: In-Line Meas. Control Met. Process. Conf., 2017.

[15] W. Jacobs, J. Shen, L. Zhou, C. Davis, P. Hunt, J. Hinton, Measurement and modelling of the EMspec® sensor response to phase transformation in 2.25 Cr-Mo steel, in: BINDT, 2018.

[16] J. Shen, L. Zhou, W. Jacobs, P. Hunt, C. Davis, Use of COMSOL® AC/DC module to model a commercial electromagnetic sensor deployed to monitor steel transformation during cooling from high temperatures, in: COMSOL Conf., 2018: pp. 22–24.